Creep Modeling in Excavation Analysis of a High Rock Slope

Jin Feng[1]; Zhang Chuhan, M.ASCE[2]; Wang Gang[3]; and Wang Guanglun[4]

Abstract: Based on the distinct element method, a numerical procedure is presented for simulation of creep behavior of jointed rock slopes due to excavation unloading. The Kelvin model is used to simulate viscous deformation of joints. A numerical scheme is introduced to create incremental contact forces, which are equivalent to producing creep deformation of a rock-joint system. The corresponding displacement of discrete blocks due to creep deformation of contact joints can be calculated by equilibrium iteration. Comparisons of results between the numerical model and theoretical solutions of a benchmark example show that the presented model has excellent accuracy for analysis of creep deformation of rock-joint structures. As an application of the model, residual deformations of the high rock slopes of the Three Gorges shiplock due to excavation unloading and creep behavior are investigated. By simulating the actual excavation process, the deformation history of a shiplock slope is studied. Good agreement has been achieved between numerical prediction and field measurements. It demonstrates the effectiveness of the presented model in analysis of the creep deformation due to excavation unloading of high rock slopes.

DOI: 10.1061/(ASCE)1090-0241(2003)129:9(849)

CE Database subject headings: Creep; Models; Slopes; Excavation; Discrete elements.

Introduction

Several numerical approaches have been developed over the past 2 decades for studying the deformation and stability of high rock slopes. The distinct element method, i.e., discrete element method (DEM) (Cundall 1980, 1988) is a powerful numerical tool for evaluating the deformation behavior and collapse process of jointed rock slopes. The functions of DEM for solving problems of deformation and stability of jointed rocks were discussed by Fairhurst and Lorig (1999). An application of DEM in dynamic analysis of high rock slopes confirms the applicability and effectiveness of DEM to predict the displacement history of a high rock slope during and after the excavation (Zhang et al. 1997). In that study, the unloading displacement histories due to excavation of the Three Gorges shiplock slopes were analyzed and compared with field measurements, which were then available up to the end of 1995. However, the creep deformation of the slopes was not included in that analysis, resulting in a significant discrepancy between numerical prediction and field measurements. It is necessary and possible to reanalyze the problem because the excavation of the shiplock slopes has been finished. Field data recorded from the measurements are now more complete, and the creep deformation can now be properly modeled by the current procedure.

Creep deformation due to rheological behavior of rock slopes is commonly analyzed using the finite element method (Ding et al. 1995) although three-dimensional finite difference modeling was also conducted by investigators to predict mining stress conditions considering the crucial creep behavior of the host strata (Gilbride et al. 2001). The rock is usually assumed as an isotropic or anisotropic continuum and only a limited number of major faults can be considered in the analysis. However, it is important to recognize that for a hard but jointed rock mass the dominant part of creep deformation is usually produced from numerous rock joints. It is, therefore, of significance to evaluate rheological behavior by using the discrete element method, which is capable of evaluating the discontinuous deformation of jointed rock. Yet, to the authors' knowledge, little work has been devoted to creep simulation in DEM for modeling deformation of high rock slopes. Based on this consideration, a creep model for jointed rock slopes is presented herein. In this paper the Kelvin model is incorporated into current DEM code and is used for creep deformation analysis of the Three Gorges shiplock slopes. For implementation of calculating creep displacements, a numerical scheme of creating incremental contact forces, which are equivalent to producing creep displacements, is developed. A detailed study on the residual deformation of the shiplock slopes using the presented method, and compared with comprehensive field measurements, has been accomplished. The results confirm the applicability of the proposed model in predicting the deformation histories of high rock slopes due to excavation unloading and creep behavior. The results also demonstrate that the unloading and creep deformation of the Three Gorges shiplock is considered to be safe for normal operation of the shiplock.

[1]Professor, Dept. of Hydraulic Engineering, Tsinghua Univ., Beijing 100084, China.

[2]Professor, Dept. of Hydraulic Engineering, Tsinghua Univ., Beijing 100084, China.

[3]Research Assistant, Dept. of Hydraulic Engineering, Tsinghua Univ., Beijing 100084, China.

[4]Professor, Dept. of Hydraulic Engineering, Tsinghua Univ., Beijing 100084, China.

Note. Discussion open until February 1, 2004. Separate discussions must be submitted for individual papers. To extend the closing date by one month, a written request must be filed with the ASCE Managing Editor. The manuscript for this paper was submitted for review and possible publication on July 10, 2001; approved on November 2, 2002. This paper is part of the ***Journal of Geotechnical and Geoenvironmental Engineering***, Vol. 129, No. 9, September 1, 2003. ©ASCE, ISSN 1090-0241/2003/9-849–857/$18.00.

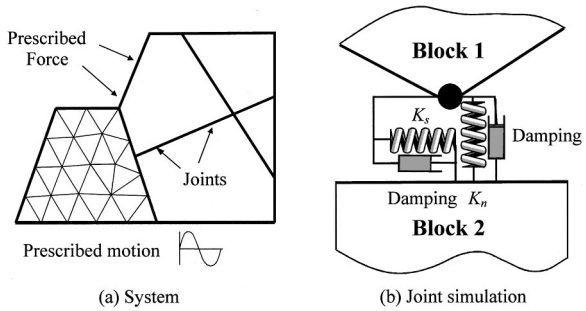

Fig. 1. Deformable distinct element method system

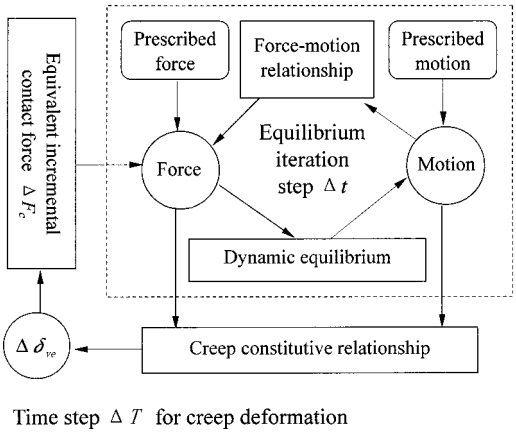

Fig. 2. Schematic flow chart of distinct element method creep model

Creep Model for Discrete Element Method

Deformable Discrete Element Method

The outstanding feature of the DEM is its ability to consider slip and separation behaviors as well as the deformation of solid blocks, in which any constitutive law for the material can be implemented. Due to its explicit time marching scheme for solving dynamic equilibrium equations and their incremental formulation of constitutive behavior in response to stress increments, DEM has an inherent suitability for nonlinear problems.

As shown in Fig. 1(a), the system is divided into blocks by contact joints. The interior regions of the deformable blocks are discretized into triangular difference meshes. The geometry of the joints can be specified individually or stochastically generated by a computer program according to statistical data from field investigation.

It is assumed that the force-displacement relationship of the joints is represented by normal and shear springs as shown in Fig. 1(b). Normal and shear dashpot elements are used for simulation of the damping mechanism of joints. The springs can be assumed to exhibit zero tension in the normal direction and follow Coulomb's friction law for shear.

The technique by Cundall (1988) to determine the deformation of the interior region of the blocks employs triangular finite difference elements of the constant-strain type. The inertial mass of each element is equally distributed to the three vertices of the element, called grid points. The elastic forces of the triangular element can be obtained from the displacements of the grids according to the constant strain assumption and constitutive law of the blocks.

In DEM solutions, damping is regarded as the dissipater of vibration energy for both static and dynamic loading. In both cases, mass- and stiffness-proportional damping may be used separately or in combination.

The solution procedure of DEM is illustrated briefly in Fig. 2. For each time step, the incremental forces acting at each grid due to deformation of the surrounding contact joints and the internal deformation of the blocks are determined from the increments of adjacent joint deformations and grid displacements as shown in the force–motion relationship box of Fig. 2. The summation of the forces F, including the stiffness damping forces, goes to the dynamic equilibrium box, where the dynamic equilibrium equations are applied, namely

$$m\ddot{u}+\alpha m\dot{u}=F+mg \tag{1}$$

where m = mass of the grid; and u = grid displacement. mg and $\alpha m\dot{u}$ represent the gravity and mass damping force, respectively.

By employing the central difference method for the acceleration on the left hand side of Eq. (1), one obtains

$$\dot{u}^{(t+\Delta t/2)}=(\dot{u}^{(t-\Delta t/2)}(1-\alpha\Delta t/2)+(F/m+g)\Delta t)/(1+\alpha\Delta t/2) \tag{2}$$

The new velocities and displacements, hence the new coordinates, are updated at each time step by Eq. (2). More details about the solution procedure can be found in references by Cundall (1980) and Zhang et al. (1997).

Creep Simulation for Discrete Element Method

Different models have been developed for simulation of creep behavior of solids. Among them, viscoelastic and viscoelastic–plastic constitutive relationships are the most common types for numerical modeling of rocks and joints. Herein, for simplicity the Kelvin viscoelastic creep model and a numerical scheme are proposed to simulate the rheological behavior of rock joints. The response of contact joints due to excavation unloading is comprised of instantaneous deformation and time-dependent viscoelastic deformation. The former can be easily obtained by using the current DEM code. For time-dependent viscoelastic deformation, the Kelvin element is introduced and incorporated into the DEM.

Figs. 3(a and b), respectively, represent the Kelvin element and loading process. When the contact force F_c is a constant and applied at $T_0=0$, the viscoelastic deformation of the Kelvin element δ_{ve} can be expressed as (Flugge 1975; Creus 1986)

$$\delta_{ve}(T)=\frac{F_c}{E}\left[1-\exp\left(-\frac{E}{\eta}T\right)\right] \tag{3}$$

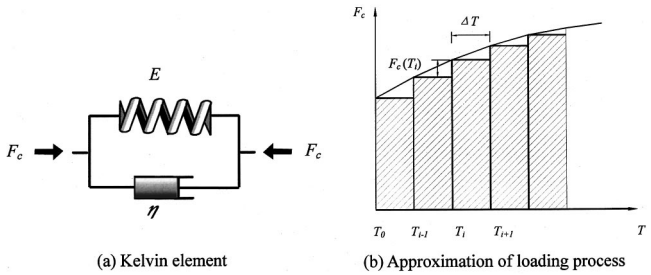

Fig. 3. Kelvin creep element

where E and η = elasticity modulus and viscosity coefficient of the Kelvin element, respectively.

For an arbitrary contact force history shown in Fig. 3(b), if the amplitude of the contact force $F_C(T_i)$ is assumed to be a piecewise constant within the time interval ΔT and thus the hereditary integral (Flugge 1975) can be adopted to calculate the accumulating normal/tangential viscoelastic deformation of joints δ_{ve} as follows:

$$\delta_{ve}(T)=J(0)F_c(T)+\int_0^T F_c(t')\frac{dJ(T-t')}{d(T-t')}dt' \tag{4}$$

where $F_c(t')$ = normal/tangential component of the contact force at time instant t'; and the integral represents the accumulating contribution of system deformation due to $F_c(t')$ within the time interval $(0,T)$; where $J(T)$ = creep compliance of the element and has the form

$$J(T)=\frac{1}{E}(1-e^{-\lambda T}) \tag{5}$$

in which $\lambda = E/\eta$.

Since the contact force and the parameters E,η are assumed to be constant during each creep time step ΔT as shown in Fig. 3(b), Eq. (3) can be expressed as

$$\delta_{ve}(T_{i+1})=\delta_{ve}(T_i)e^{-\lambda\Delta T}+\frac{1}{E}F_c(T_i)(1-e^{-\lambda\Delta T}) \tag{6}$$

and the incremental form as

$$\Delta\delta_{ve}(T_{i+1})=\Delta\delta_{ve}(T_i)e^{-\lambda\Delta T}+\frac{1}{E}\Delta F_c(T_i)(1-e^{-\lambda\Delta T}) \tag{7}$$

$$\Delta\delta_{ve}(T_0)=0 \tag{8}$$

where

$$\Delta F_c(T_i)=F_c(T_i)-F_c(T_{i-1})$$

$$\Delta\delta_{ve}(T_i)=\delta_{ve}(T_i)-\delta_{ve}(T_{i-1})$$

$$\Delta T=T_{i+1}-T_i$$

Solution Scheme

In the equilibrium iteration of the discrete element system, as described in Cundall (1980) and Zhang et al. (1997), the main calculation cycle consists of applying the law of motion to all grid points followed by the calculation of force increments from displacement increments for all spring-like elements (contact springs, continuum triangle meshes, etc). To maintain the convergence of such an explicit time marching scheme, the time step Δt for equilibrium iteration normally falls into the range of $10^{-3}-10^{-5}$ s. However, the creep deformation of rock joints is a much longer time process and one time step for creep calculation ΔT may be days, weeks, or even months. Thus, the calculation cannot be efficiently conducted by simply using the same iteration process. Herein, Δt denotes the explicit time marching step for discrete rock deformation due to unloading, and ΔT stands for the time step for computation of creep deformation.

Herein, a method is presented for calculation of incremental contact forces, which are equivalent to producing the deformation due to creep behavior.

Let us define the equivalent incremental contact force $\Delta F_c(T_{i+})$ at T_{i+}

$$\Delta F_c(T_{i+})=-K\cdot\Delta\delta_{ve}(T_{i+1}) \tag{9}$$

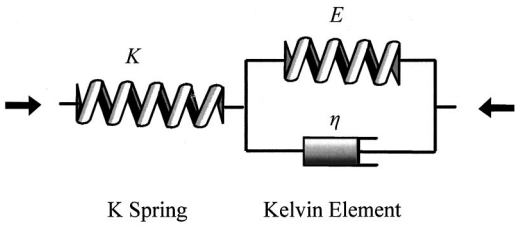

Fig. 4. Three parameter model for joint simulation

where $\Delta\delta_{ve}(T_{i+1})$ is determined by Eq. (7); and K = normal or shear stiffness of contact joints (i.e., K_n or K_s).

For each creep time step ΔT_i, the equivalent incremental force from Eq. (9) is added to the previous contact force $F_c(T_i)$, i.e.,

$$F_c(T_{i+})=F_c(T_i)+\Delta F_c(T_{i+}) \tag{10}$$

and the equilibrium iteration will automatically be carried out to produce the creep displacements for the whole system.

For DEM with unloading and creep deformation, the contact joint is physically represented by a three-parameter model (K,E,η) with a spring and a Kelvin element in series shown in Fig. 4. The instantaneous deformation of the joint is simulated by a K spring, which may slip or break or open under some conditions. The Kelvin element therein accounts for the viscous creep deformation although it is, in reality, calculated through the equivalent incremental forces via a K spring-block node system. The details of the solution scheme are illustrated in Fig. 2, and the following computation steps are summarized:

1. Unloading deformation: At the initial time step, when the prescribed forces (including excavation unloading and self weight) are applied to the nodes, the system starts to move due to these unbalanced forces and the dynamic equilibrium Eq. (1) is performed for each node of the system. Since the unloading forces are imposed as step functions on the excavation surface, the system starts with an oscillating response. Thus, the computational steps are marching and the equilibrium iterations are repeated until the response becomes stable (achieves new balance). The new coordinates of nodes are continuously updated and the instantaneous deformation of the system due to unloading can be obtained. This step of

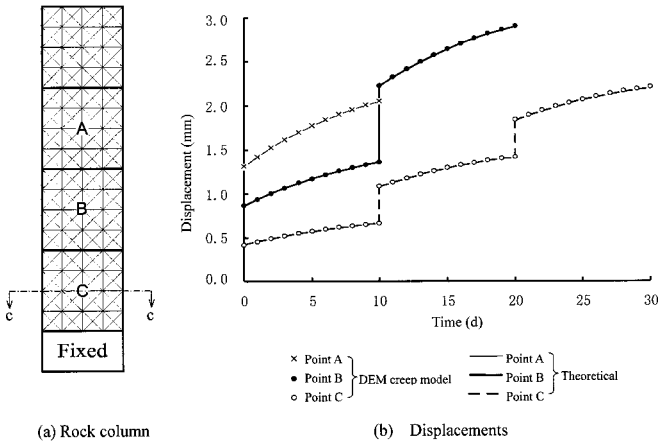

Fig. 5. Comparison of displacements between numerical model and theoretical solutions

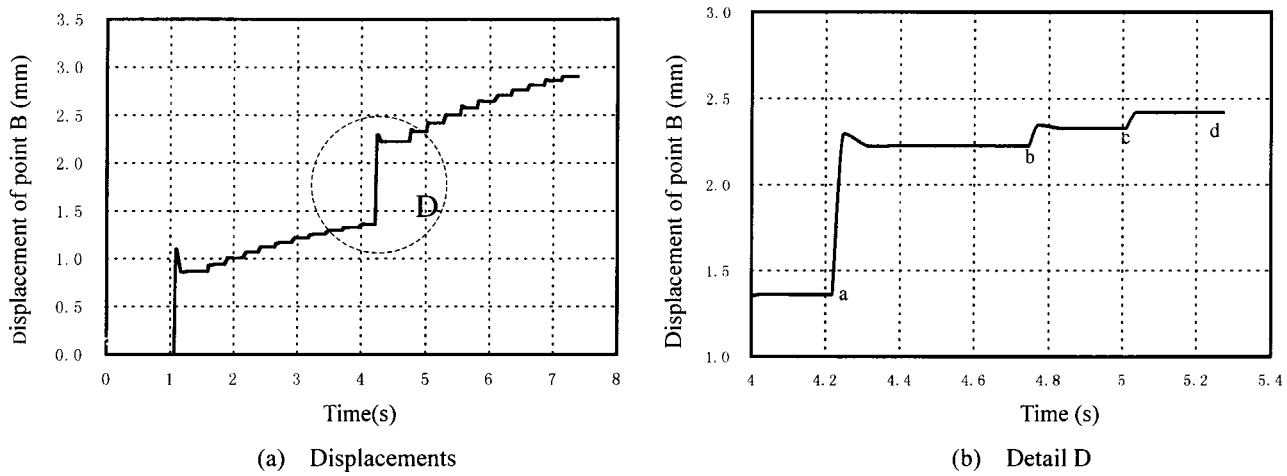

Fig. 6. Abrupt changes of displacements due to unloading and creep

computation proceeds within the dashed frame in Fig. 2 using a very small time step Δt.

2. Creep deformation: For time step of creep deformation T_i to T_{i+1}, Eqs. (7)–(10) are used to calculate the equivalent incremental contact forces ΔF_c and the corresponding updated contact forces $F_c(T_{i+})$ due to creep deformation. These abruptly changing forces bring the system into a newly unbalanced status, and the dynamic equilibrium iterations are again carried out until a new balance status is reached after a certain number of time steps Δt. The coordinates of the system are then updated and the deformation due to creep behavior can be obtained. This step of computation is accomplished repeatedly in and out of the dashed frame of Fig. 2, where the computation of the equivalent incremental contact forces ΔF_c proceeds outside the dashed frame using the time step ΔT for creep deformation. After ΔF_c is obtained, it reenters into the dashed frame for further calculation until newly updated coordinates are reached.
3. Repeat steps 1 and 2 until the unloading process is finished and the creep behavior vanishes in the sense of a prescribed tolerance.

Verification

To demonstrate the validity of the proposed numerical model and the solution scheme for creep deformation, a rock column consisting of four 10 m×10 m square blocks shown in Fig. 5(a) is studied. Each block is further divided into triangular elements to account for elastic deformation. The rock parameters in the analysis are: mass density $\gamma_r = 2{,}750$ kg/m^3; elastic modulus $E_r = 4\times10^{10}$ Pa; and Poisson's ratio $\nu = 0.22$. The joint parameters are: normal stiffness $K_n = 6.9\times10^8$ Pa; parameters for Kelvin creep element are: $E = 6.9\times10^8$ Pa; and $\eta = 6.9\times10^9$ Pa day. An unloading and creep test is conducted as follows: assume that the first, second, and the third block are, respectively, removed at the very beginning instant of the 1st, 10th, and 20th day. The vertical displacement histories of points A, B, and C at the center of the second, third, and fourth blocks, respectively, are examined. The time step ΔT for creep calculation is taken to be 1 day, while the Δt used in the dynamic equilibrium iteration is 1.318×10^{-4} s. Fig. 5(b) shows a comparison of displacement histories between the proposed model and the theoretical solutions for the corresponding 1D column solved by hand (Creus 1986).

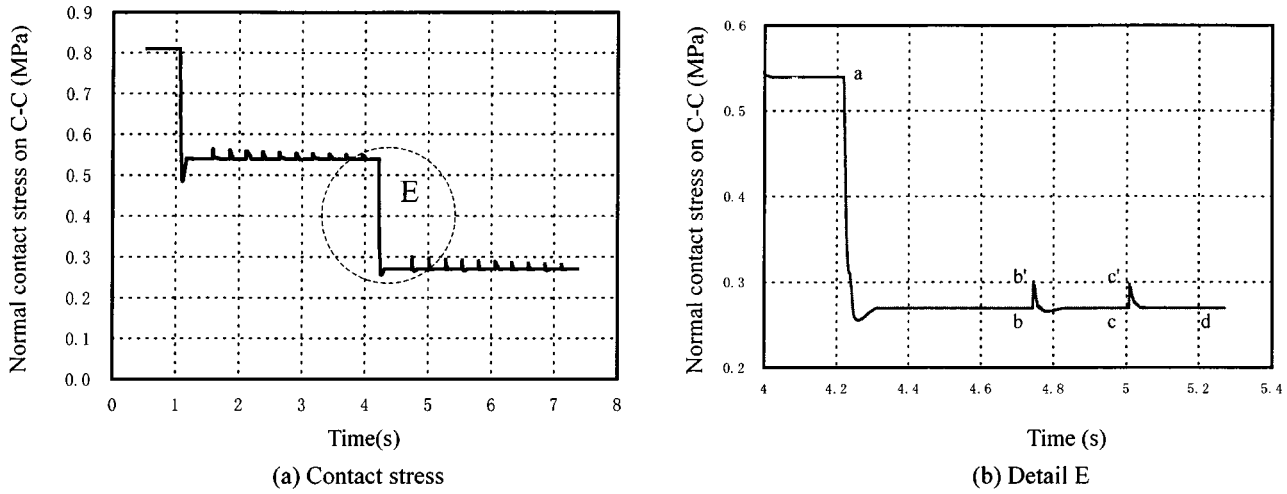

Fig. 7. Abrupt changes of normal contact stresses due to unloading and creep

Excellent agreement between the two has been observed, indicating the applicability and accuracy of the method to account for the unloading deformation and creep behavior. From Fig. 5(b), it is interesting to see that the unloading displacements of points A, B, and C, respectively, occur abruptly at the very beginning of the 1st, 10th, and 20th day, demonstrating the instantaneous pattern of unloading displacements. However, the creep displacements at each point increase gradually day by day showing continuous creep deformation.

To illustrate the solution scheme of the equivalent incremental contact force method, Figs. 6 and 7 show the histories of displacements of point B and the contact stresses on the cross section $C-C$ after the removal of the first and second blocks of the column. Note that they are now drawn in a computational time scale to examine the mechanism of the equivalent incremental contact forces and the corresponding creep deformation. It is shown in Fig. 7 that in addition to the contact stress drops produced by unloading blocks, ten small pulses of contact stress each between the two unloading events are evident. These stress pulses represent the effects of equivalent incremental contact forces due to creep deformation, and they all vanish after a new equilibrium status is reached. Corresponding to these stress pulses, a number of displacement increments occur as shown in Fig. 6, representing the gradually occurring creep deformation, although they appear in a pattern of step increments in the computational time scale.

Application to Three Gorges Shiplock Slopes

Basic Condition

The shiplock is located on the left bank of the Three Gorges dam site on the central reaches of the Yangtze River in China. It is a double-channel shiplock with five stages and a total length of 6,442 m, including the 4,800 m upstream and downstream approach channels. Each shiplock chamber has dimensions of $240\times34\times5$ m (length×width×minimum water depth) sufficient to accommodate a 5,000 t barge fleet, with a total water head of 113 m. More details of the project can be found in Zhang et al. (1997). For evaluation of stability against sliding and deformation of the shiplock, Zhu et al. (1999) also studied the problem using finite element method and DEM, but the time effects due to creeping were not considered. In the field measurement, three cross

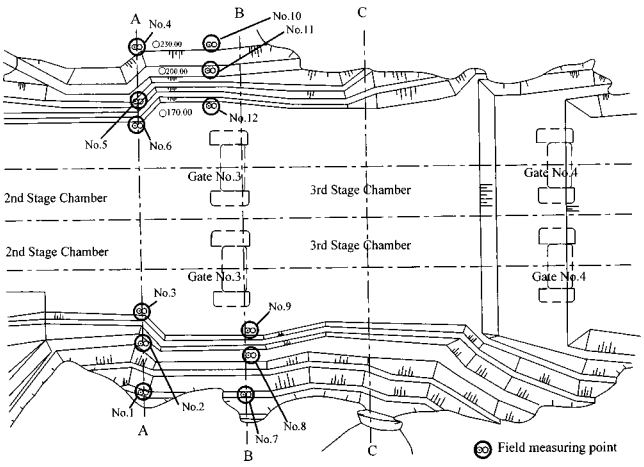

Fig. 8. Plan view of excavation and field measuring points (see Figs. 13 and 14 for results)

sections along the channel are selected for installation of measuring apparatus. Two typical cross sections $A-A$ and $B-B$ of the shiplock slopes are analyzed by the presented model. A plan view of the excavation of the shiplock and the field measurement points are shown in Fig. 8, and the excavation cross section $A-A$ and its joint discretization are shown in Figs. 9 and 10, where the maximum height of the slope excavation reaches approximately 120 m. According to field investigation and geological exploration, the chief statistical parameters of the joint structures including dip bearing, dip angle, and length were obtained. In the statistical process, normal and lognormal distributions are assumed for dip parameters and length, and negative exponential distributions are assumed for the space intervals. The resulting data allowed a system of joints to be generated using stochastic network generation. To consider the strength difference between the joints and rock bridges, a weighted averaging method is employed to obtain the overall shear strength of the equivalent continuous joint system shown in Fig. 10. Detailed information of the method and parameters obtained can be found in Zhang et al. (1997). Because the residual deformation of the chamber wall due to static unloading and creep may affect normal operation of the gate facilities and needs to be studied, a large amount of field deformation measurements have been taken. As shown in Fig. 8, 12 measuring

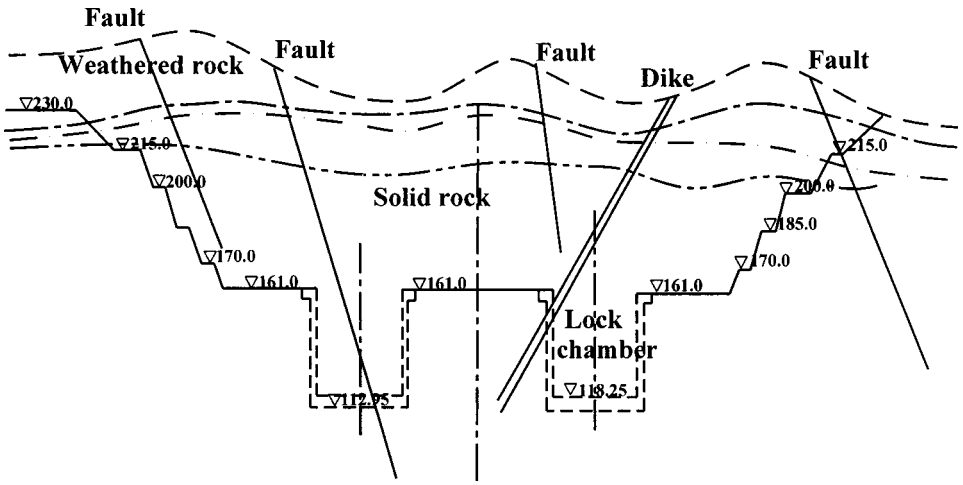

Fig. 9. Cross section of Three Gorges shiplock (elevation in m)

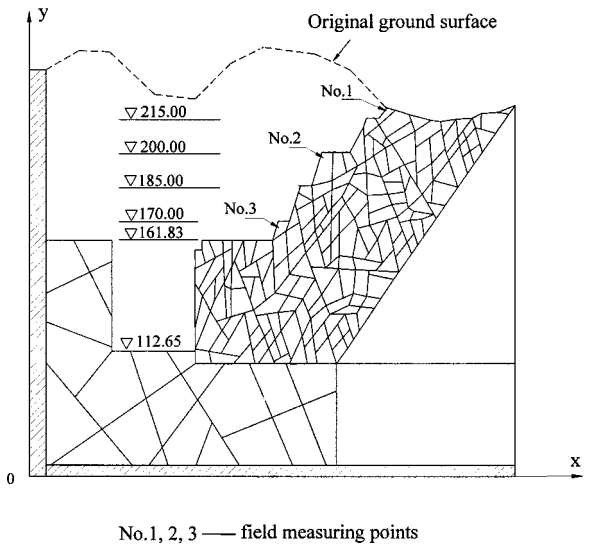

Fig. 10. Joint discretization for cross section $A-A$ (south slope)

points at different elevations are chosen for comparison analysis between the numerical results and field measurements. The mechanical properties of rock and joints are based on data from comprehensive tests and measurements: both laboratory and field. The most important parameters used in the analysis are listed in Table 1. A view of the excavated shiplock slope is shown in Fig. 11.

Determination of Creep Parameters

As mentioned previously, the total deformation of the system consists of two parts, namely: (1) the instantaneous deformation due to the rock mass and joints, in which only the linear elastic portion is considered; and (2) creep deformation. As shown in Fig. 3 the total displacements $\delta_0(T)$ can be described as

$$\delta_0(T)=\frac{F_c}{K}+\frac{F_c}{E}[1-e^{-\lambda T}] \tag{11}$$

where $\delta_0(T)$ represents the total displacements and also has the form

$$\delta_0(T)=\delta_e+\delta_{ve}(T) \tag{12}$$

in which δ_e and $\delta_{ve}(T)$ = instantaneous and creep displacements, respectively. The form of the time history of $\delta_0(T)$ may be depicted in Fig. 12, where we assume that the creep displacements converge approximately at $T=T_c$, i.e.,

$$\delta_{ve}(T_c)\approx\delta_{ve}(\infty) \tag{13}$$

Table 1. Mechanical Properties of Rock and Joints

Rock type	Elastic modulus E_r (GPa)	Poisson's ratio ν	Mass density ρ (kg/m^3)	Joint stiffnesses (MPa)	
				K_n	K_s
Fresh and microweathered rock	20–40	0.22	2,750	690	280
Minor-weathered rock	12–17	0.24	2,700	240	96

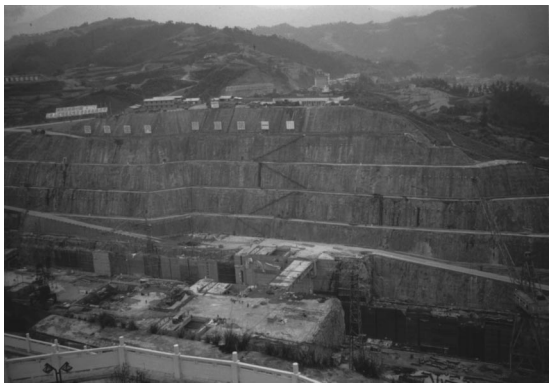

Fig. 11. View of excavated shiplock slope

According to the field measurements, it appears that the time period of T_c can be taken as 1 year, which is sufficient for convergence of creep deformation.

Combining Eqs. (11), (12), and (13) yields the following equation for creep parameter E:

$$E=K\frac{\delta_e}{\delta_0(T_c)-\delta_e} \tag{14}$$

where K represents the joint stiffness, i.e., K_n, K_s, which are obtained from field or laboratory tests. The field tests for obtaining joint stiffness were conducted in drainage adits at different elevations. Rock columns with specific seams were excavated. Compression plate tests with an area of 500 mm$\times$600 mm were performed. Normal and shear loads were imposed, respectively, and corresponding displacements were measured and the load–displacement relationships are obtained. From the test results and corresponding computational simulation for the tests, parameters K_n, K_s can be obtained, and their mean values are listed in Table 1.

Determination of another parameter η depends on the asymptotic behavior of creep displacement curve from the field measurements. In situ and laboratory shear tests for rheological parameters of the rock joints were comprehensively conducted (Xia et al. 1996). It is concluded that the curve shapes of the creep displacements depend on local rock joint conditions and the normal and shear loading levels. Herein, considering the complicated conditions of the Three Gorges shiplock slope, the DEM back analysis from the field measurements of the displacement histories of the slope are carried out for determination of the

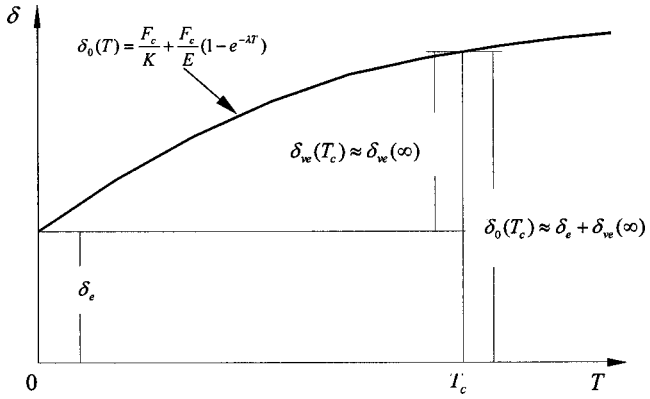

Fig. 12. Displacement history for three parameter mode model

Table 2. Creep Parameters of Joints

Parameter	Values	
	Tangential direction	Normal direction
E (MPa)	1,400	480
η (MPa day)	168,000	57,600

equivalent parameters E and η. Since the data from the field measurements at the site of the shiplock slope are available during the complete excavation process, repeated back analyses were conducted to obtain equivalent creep parameters, which are thus better fitted with the field measurements. The final creep parameters are listed in Table 2.

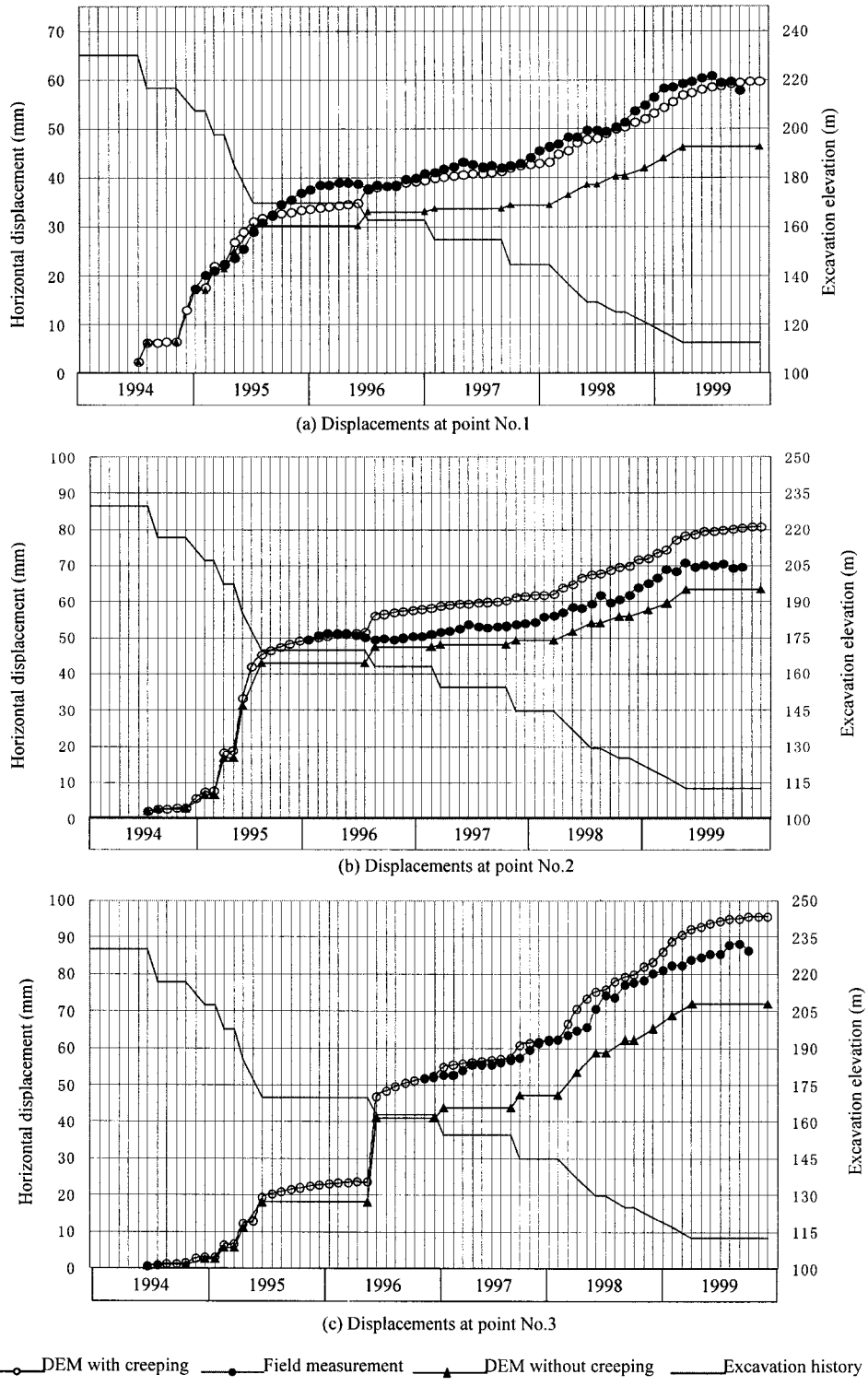

Fig. 13. Comparison of displacements between numerical results and field measurements (cross section $A-A$ south slope)

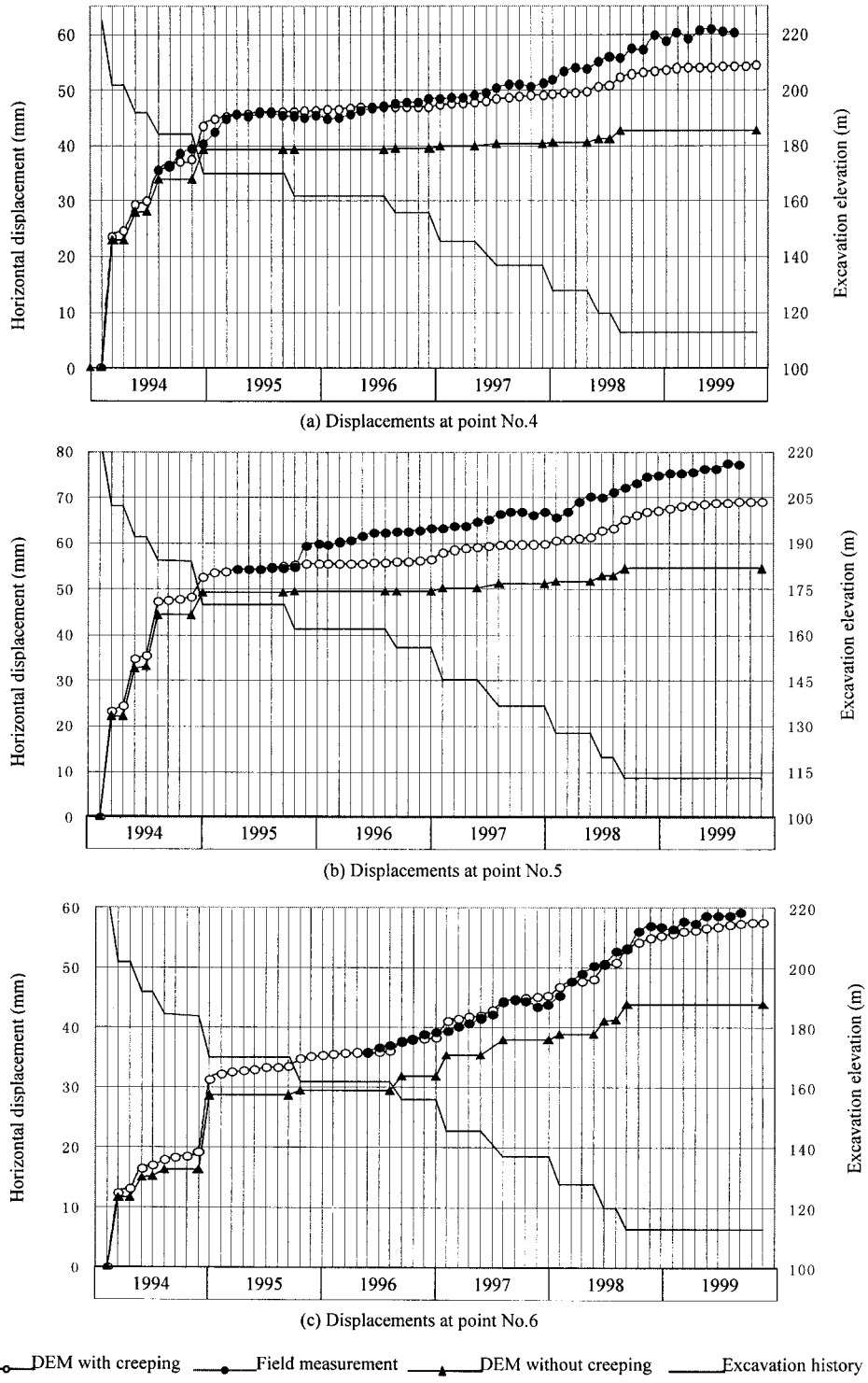

Fig. 14. Comparison of displacements between numerical results and field measurements (cross section $A-A$ north slope)

Comparison of Numerical Results with Field Measurements

The comparison of displacements of the shiplock slope between numerical results and field measurements are shown in Figs. 13–14, where the numerical results with and without considering creep deformation are presented for comparison with the field measurements. To investigate the residual and creep deformation during the construction process, and monitor stability during the excavation stages, comprehensive field measurements were conducted, which included 144 surveying stations and 12 inclinometer holes at different elevations of the slope and the drainage tunnels. Both the surface and interior deformation of the slopes were measured. Also included in the same figures are excavation histories from which the instantaneous pattern of displacements due to the unloading effects is vividly shown. Some observations can be summarized from the results.

1. The proposed model of creep deformation added into DEM code is applicable to analysis of creep deformation of jointed

rock slopes provided the creep parameters from field measurements or tests are available for the analysis.

2. Considering the complicated geological conditions and excavation process, the overall agreements between the numerical results and field measurements are very good when the creep deformations are considered. However, a parallel discrepancy is evident for all measuring points between the DEM results and field measurements if the creep deformations are ignored in the analysis. This indicates that the creep behavior must be taken into account in deformation analysis of a jointed rock slope.
3. As shown in Figs. 13 and 14, the excavation of the Three Gorges shiplock slopes started from mid 1994 and was finished around the end of 1999. Corresponding field measurements have been consecutively conducted for 3–5 years. Since different elevations for measuring points are selected, the field measurements for a specific point can only be commenced after the excavation reaches the elevation of that point. As observed from curves of black circles for field measuring displacements shown in Figs. 13–14, the relative recorded displacements are in a range of 20–40 mm for different points of section $A-A$. Similar results for section $B-B$ are also obtained but not shown herein for space limitation. From the results, the total predicted displacements from numerical analysis reach 60–90 mm, in which displacements of about 20–50 mm occur before the excavation reaches the corresponding elevation. Considering that the creep deformations have basically converged the engineering significance of the relative measuring displacements is not important regarding the stability of the slopes and safe operation of the gate facilities.

Conclusions

A creep model for analysis of jointed rock deformation is presented and has been incorporated into the existing DEM code. The Kelvin element is employed to describe the behavior of creep deformation, and a method of equivalent incremental contact force is used for numerically triggering the occurrence of creep displacements. Verification of an existing example shows that excellent accuracy can be achieved in the prediction of the creep development of jointed rock.

As an important engineering application of the proposed model, the displacement histories of the Three Gorges shiplock slopes due to excavation unloading are analyzed. The results are compared with the comprehensive field measurements. Good agreement between the two is confirmed when creep deformations are included in the analysis. This indicates the applicability of the proposed model for evaluation of slope deformation due to excavation unloading and creep behavior. The results also demonstrate that the unloading and creep deformation of the Three Gorges shiplock is considered to be safe for normal operation of the shiplock.

Acknowledgments

The writers gratefully acknowledge the financial support and the field measurement data for this work, which was supported by the China Three Gorges Engineering Development Corporation. Many thanks go to Professor Zhang Chaoran and Professor Yu Sanda, the Chief Engineer and the Project Director of the Corporation for their kind support for providing field measurement data. Appreciation is also given to Dr. Xu Yanjie and Mr. Zhou Qingke for their assistance.

References

Creus, G. J. (1986). ''Viscoelasticity-basic theory and applications to concrete structures.'' *Lecture notes in engineering*, C. A. Brebbia and S. A. Orszag, eds., Springer, Berlin.

Cundall, P. A. (1980). ''UDEC—A generalized distinct element program for modeling jointed rock.'' *Final Technical Rep. No. DAJA37-39-C-0548, to European Research Office*, U.S. Army.

Cundall, P. A. (1988). ''Formulation of three-dimensional distinct element model, Part I, A scheme to detect and represent contact in system composed of many polyhedral blocks.'' *Int. J. Rock Mech. Min. Sci. Geomech. Abstr.*, 25(3), 107–116.

Ding, X., Xu, P., and Xia, X. (1995). ''Unloading deformation and creep analysis of the Three Gorges shiplock slopes due to excavation.'' *J. Yangtze River Scientific Research Institute*, 12(4), 37–43 (in Chinese).

Fairhurst, C., and Lorig, L. (1999). ''Improved design in rock and soil engineering with numerical modeling.'' *Distinct element modeling in geomechanics*, V. M. Sharma, K. R. Saxena, and R. D. Woods, eds., Balkema, Rotterdam, The Netherlands, 27–46.

Flugge, W. (1975). *Viscoelasticity*, Springer, New York.

Gilbride, L. J., Agapito, J. F. T., and Hollberg, K. F. (2001). ''Time-dependent stability implications for planned two-seam mining at the OCI Wyoming, L. P. Big Island trona mine.'' *Proc., 38th U.S. Rock Mechanics Symp.*, D. Elsworth, J. P. Tinucci, and K. A. Heasley, eds., Lisse, Balkema, Rotterdam, The Netherlands, 1539–1546.

Xia, X., Xu, P., and Ding, X. (1996). ''Creep behavior of rock and stability and rheological analysis of high slopes.'' *Chin. J. Rock Mech. Eng.*, 4, 312–322 (in Chinese).

Zhang, C., Pekau, O. A., Jin, F., and Wang, G. (1997). ''Application of distinct element method in dynamic analysis of high rock slopes and blocky structures.'' *Soil Dyn. Earthquake Eng.*, 16, 385–394.

Zhu, W., Zhang, Q., and Jing, L. (1999). ''Stability analysis of the shiplock slope of the Three Gorge Project by three-dimensional FEM and DEM techniques.'' *Proc., of ICADD-3, 3rd Int. Conf. of Analysis of Discontinuous Deformation*, Vail, Col. 263–272.